



**HAL**  
open science

## Performance enhancement of concentrated photovoltaic systems CPVS using a nanofluid optical filter

Afef Jannen, Monia Chaabane, Hatem Mhiri, Philippe Bournot

### ► To cite this version:

Afef Jannen, Monia Chaabane, Hatem Mhiri, Philippe Bournot. Performance enhancement of concentrated photovoltaic systems CPVS using a nanofluid optical filter. *Case Studies in Thermal Engineering*, 2022, 35, pp.102081. 10.1016/j.csite.2022.102081 . hal-04061592

**HAL Id: hal-04061592**

**<https://amu.hal.science/hal-04061592>**

Submitted on 7 Apr 2023

**HAL** is a multi-disciplinary open access archive for the deposit and dissemination of scientific research documents, whether they are published or not. The documents may come from teaching and research institutions in France or abroad, or from public or private research centers.

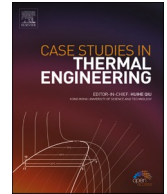
L'archive ouverte pluridisciplinaire **HAL**, est destinée au dépôt et à la diffusion de documents scientifiques de niveau recherche, publiés ou non, émanant des établissements d'enseignement et de recherche français ou étrangers, des laboratoires publics ou privés.



Distributed under a Creative Commons Attribution 4.0 International License

Contents lists available at [ScienceDirect](https://www.sciencedirect.com)

# Case Studies in Thermal Engineering

journal homepage: [www.elsevier.com/locate/csie](http://www.elsevier.com/locate/csie)

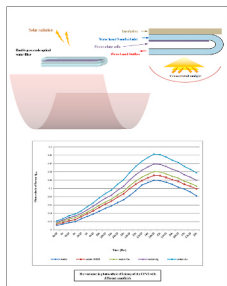
## Performance enhancement of concentrated photovoltaic systems CPVS using a nanofluid optical filter

Afef Jannen<sup>a,\*</sup>, Monia Chaabane<sup>a</sup>, Hatem Mhiri<sup>a</sup>, Philippe Bournot<sup>b</sup>

<sup>a</sup> Laboratory of Thermal and Thermodynamic Industrial Processes, Department of Energy Engineering, National Engineering School of Monastir, Monastir University, Ouardanine Road, 5000, Monastir, Tunisia

<sup>b</sup> Aix Marseille Univ, CNRS, IUSTI, Marseille, France

### GRAPHICAL ABSTRACT



### ARTICLE INFO

#### Keywords:

Concentrating photovoltaic system CPVS  
CFD simulations  
PV cooling  
Optical water filter  
OWF  
Performance optimization  
Nanofluid filter

### ABSTRACT

The exploitation of solar energy using hybrid photovoltaic/thermal (PVT) system can represent a viable choice for the rising energy demand. Due to the wide range of PVT applications, many designs have been developed to improve the solar system global performance by cooling PV cells. The proposed system offers a practical heat gain in addition to the electrical efficiency enhancement. The integration of optical water filters (OWF) in photovoltaic systems could be an advantageous solution for their performance improvement. In this work, three different optical water filter models are evaluated using Cinematic fluid dynamics CFD modeling and their effect on the global system operating is discussed. Three shapes of OWF models are considered. Model (I) is an OWF under the PV cell. Model II is an OWF which passes over and under PV cells with separated inputs. Model III consists of a double pass mode OWF. Results showed that the maximum photovoltaic efficiency is corresponding to model (III) and reaches 12.08% at 14 h. The paper highlighted the different impacts associated with different OWF models. The results showed a significant increase in water outlet temperature. Consequently, an enhancement of the PVT

\* Corresponding author.

E-mail address: [afef.jannen@hotmail.fr](mailto:afef.jannen@hotmail.fr) (A. Jannen).

<https://doi.org/10.1016/j.csie.2022.102081>

Received 22 February 2022; Received in revised form 21 April 2022; Accepted 29 April 2022

Available online 4 May 2022

2214-157X/© 2022 The Authors. Published by Elsevier Ltd. This is an open access article under the CC BY license (<http://creativecommons.org/licenses/by/4.0/>).

system thermal efficiency is achieved. Finally, various water-based nanofluid (Al<sub>2</sub>O<sub>3</sub>, Cu, Ag, Au) optical filters are elucidated. The optimal photovoltaic performance is obtained by the water-Au nanofluid which allowed an electrical efficiency varying between 2% and 10%. Nanofluid filters have thus been shown to improve the performance of the CPVS concentrated photovoltaic system, not only because of the thermodynamic properties but also as a spectrally separated cooling system.

**Nomenclature**

*Symbol*

- G Solar irradiance, W/m<sup>2</sup>
- h Convective heat transfer coefficient, W/m<sup>2</sup>K
- k Turbulent kinetic energy, m<sup>2</sup> s<sup>2</sup>
- CP Specific heat, kJ/kg K
- $\dot{m}$  water mass flow rates, l/s
- T Temperature, °C
- g gravitational acceleration, m/s<sup>2</sup>

*Greek letter*

- $\eta_{el}$  electrical efficiency
- $\eta_{th}$  thermal efficiency
- $\lambda$  thermal conductivity, W/m K
- $\rho$  density, kg/m<sup>3</sup>
- $\beta$  thermal expansion coefficient, K<sup>-1</sup>

*Subscripts*

- amb ambient
- el electrical
- th thermal

*Abbreviations*

- CFD Cinematic fluid dynamics
- PV photovoltaic
- PV/T Photovoltaic thermal
- CPVS Concentrator photovoltaic system
- OWF Optical water filter

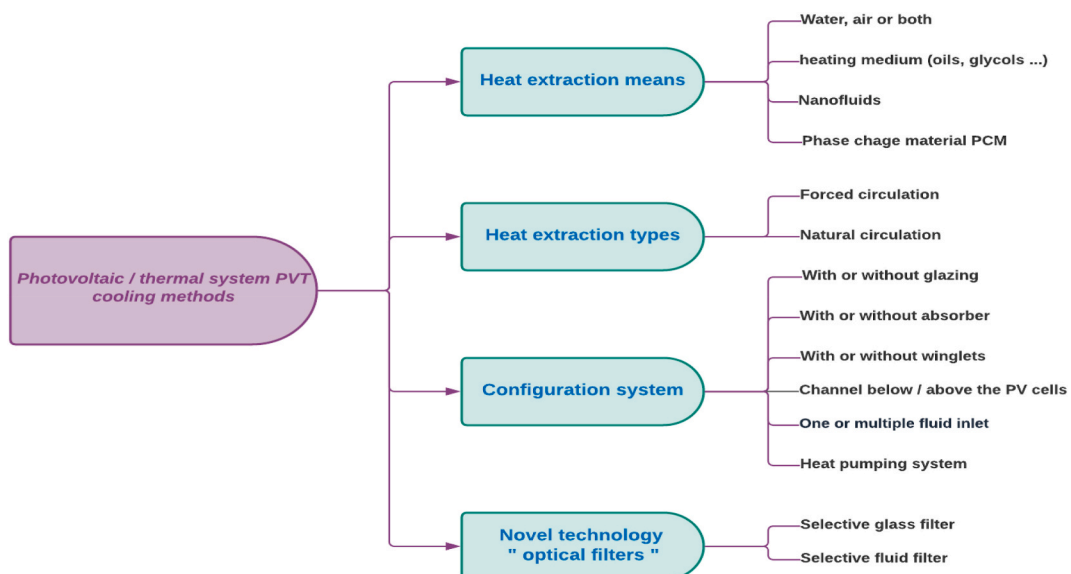


Fig. 1. Classification of PV/T cooling systems.

## 1. Introduction

The exponential population growth leads to the increasing need for energy consumption. This increase is accompanied by environmental problems due to the excessive use of non-renewable energy resources. For that solar energy is needed not only to cope with the soaring demand but also because it's a clean source which is no harmful environmental effects [1]. Many researchers have developed various technologies to harvest solar energy using photovoltaic processes [2]. Despite the multiple advantages of photovoltaics, it can convert only about 15 to 20% of the captured sunlight into electricity while the remaining turns into heat [3]. The photovoltaic system is heated as a result of indirect absorption with continuous work [4]. Solar cell efficiency is considerably affected by the PV cell's temperature increase as the electrical efficiency of any PV panel is inversely proportional to the temperature of the solar cell [4]. Applying a cooling system may be one way to reduce this drawback. Photovoltaic thermal PVT systems are generally classified according to the layout of the heat extraction [5], the working environment, and the final application [6].

In addition, PVT systems can be classified on the basis of their mounting into non-concentrating and solar-concentrating systems. A broad classification of PVT cooling systems is illustrated in Fig. 1, which will be discussed in more detail. Many researchers have been interested in these solar systems in recent years, and various designs of PV cooling system methods have been discussed. Researchers in this area are making incessant progress in discovering methods to cool photovoltaic cells [8], which are also classified into active and passive cooling techniques.

Passive cooling techniques are classified into three main categories: passive cooling of the air; heat pipe; or sink. The heat sinks are indeed highly thermally conductive materials. Ahmed et al. [9] carried out a numerical simulation that looks at the thermal performance of truncated multi-level fin heat sinks (MLFHS) profiles for PV cooling with natural convection. The concept is based on preventing stagnation in the fin restricted area, or exchanger, to drive natural convection cooling [10]. Water immersion cooling is another passive cooling technique reported in the literature [7]. When the appropriate submersion depth is used, this method significantly reduces PV the module temperature and boosts the photovoltaic efficiency.

PCMs are materials that retain thermal energy to stabilize temperature. PCMs absorb latent heat when their physical state changes [11]. The advantage of passive cooling is that, by limiting the size of the cooling system at high concentrations, the installation costs of HCPV hybrid concentrator photovoltaic systems are considerably reduced [12]. Nevertheless, this temperature decrease must be meticulously planned to keep heat sink costs to a minimum [13]. Besides, PCMs are substances that can continue to maintain thermal energy. A simulation was used to study PCM cooling techniques by Karthick et al. [14], who analyzed the maximum and average increase in power gain obtained for the PV-PCM panel. According to the final, the power output of the PV panel with PCM was shown to be higher at 96.55 Whr. Even PCM could be a resourceful solution to reduce temperature and so to cool PV cells [15]. But the main disadvantages of using PCMs are related to their long-term degradation by reactions with other materials. These reactions are like oxidation, hydrolysis and thermal decomposition [16].

Active cooling requires a coolant that requires a fan or a pump power in order to control and maintain the system operating [17]. Extensive research has been conducted in this area, and the primary coolant used is air and other fluids such as water or glycols. Active air cooling (forced air circulation) is considered as an effective PV panel cooling technique. Tonui et al. [18] carried out a study on the improvement of heat extraction by low-cost modifications of their PV/T air system's channels. The water immersion cooling technique is another active PV cooling method. This consists of installing PV panels underwater [19]. Despite its low environmental impact and high-temperature significant decrease potential, immersion cooling is not applicable to floating solar systems [20].

Previous research has shown that active water cooling is the most simple and productive cooling technique, and it should be investigated further. However, active water cooling is not always feasible. For active water cooling to be meaningful, the environment must have a consistent supply of cool water and the array to be cooled should be large enough to offset the energy consumption [21]. For that, scientists developed spectrum filter cooling (optical beam splitter) as a novel and sophisticated cooling method [22]. Various liquids could be used in PV systems as selective absorbing fluids or as optical filters [23]. The main objective of optical filters is to separate the useful wavelengths for photovoltaic conversion from the unwanted wavelengths, which leads to a rise in PV cell temperature. The redundant wavelengths are filtered out for thermal uses. The principal cause of the increased temperature is that the PV cells cannot convert all direct sunlight to electricity, so some of it is transformed into heat. Solar radiation has three spectra: 8% ultraviolet UV (from 0.2 to 0.38  $\mu\text{m}$ ), 36% visible VIS (from 0.38 to 0.78  $\mu\text{m}$ ), and 46% infrared IR (from 0.78 to 2.5  $\mu\text{m}$ ) [24]. Furthermore, the thermophysical properties of silicon photovoltaic cells prove that the cells use the VIS and even some of the IR to generate electricity. However, the UV and the rest of the IR are wasted and converted into heat in the cells. This heat brings down the efficiencies of the PV panel. As a result, the optical filter absorbs the majority of the IR once it reaches the PV module. Compared to a conventional PV module, this leads to limiting the percentage of the heat generated in the PV cells and reducing cell temperatures.

The optical liquid filter is composed of two main loops: thermal and electrical. The electrical loop consists of the PV panel. The thermal loop is made up of a liquid tank with a high transmittance glass cover, which has the same length as the PV module. Al-Shohani et al. [25] performed new experimental studies aimed at reducing heat accumulation in a photovoltaic module by an optical water filter OWF with a thickness ranging from 1 to 5 cm. The OWF is placed above the photovoltaic module and is used to, at once, transmit the visible spectra VIS to the photovoltaic module for electricity production and absorb the unwanted infrared spectra IR and convert them to heat for domestic usage. The results show that there is a significant effect of the thickness of the water layer on the reduction of the temperature of photovoltaic cells (14–30.2%). Similarly, many researchers, such as Yazdanifard et al. [5] and Looser et al. [26], have used these liquid optical filter beam fractionation methods. Thanks to their characteristic infrared absorption spectrum, glycol,

mineral oil, and liquid salt have demonstrated their precursory feasibility in dividing the solar spectrum into thermal and electrical applications.

Wang et al. [27] described a new design of a revolutionary solar PVT system using a Fresnel Reflector Linear Concentrator (LFR) and a nanofluid optical filter. The analysis of the system measurement shows that increasing the inlet nanofluids flow velocity as well as the ambient temperature or decreasing the inlet nanofluids temperature or convection heat transfer coefficient, can enhance the thermal efficiency of the PVT system. Recently, Mostafa et al. [28] established a numerical model of a concentrator photovoltaic thermal system PVC/T using a liquid spectral filter. The effect of PV cell selectivity on the performance of the CPV/T system is evaluated for varying solar concentration ratios (CR) depending on the thermal and optical characteristics of the liquid filters. It's concluded that the ideal optical water filter is obtained under high CR, which allows the best total energy efficiency of the system. Nevertheless, at low CR, the spectral absorbance of the fluid filter should be increased throughout the intercepted spectrum. At the same time, in terms of exergy efficiency, it is preferable to apply a fluid with a higher spectral permeability in order to utilize a wider area of the solar spectrum. As a result, the ideality of thermo-optical properties is mostly determined by the operating circumstances as determined by the aforementioned selection criteria.

On the other hand, the usual fluids like water and oils are not very effective in the PV/T system due to their thermal conductivity and heat carrying capacity, which are relatively low [21]. That's why researchers are focusing on different kinds of fluid with enhanced thermal conductivity and heat carrying capacity: nanofluids. By dint of these properties, nanofluids are the best option for photovoltaic cooling [29]. Nano-particle fluids also appear to be an occasion for liquid-absorbing photovoltaic/thermal systems [19]. Radwan et al. [30] came up with a new concept for a concentrated PV/T system employing a microchannel heat sink with nanofluid. Various concentrations of Al<sub>2</sub>O<sub>3</sub>/water and SiC/water nanofluids were considered, which were used as refrigerants. The researchers concluded that the temperature of solar cells is shortened to a higher concentration ratio of nanofluid compared to water. Using water-based and SiC nanofluids, a computational and experimental study was undertaken by Kazem et al. [31] to evaluate the enhancement of a Web configuration PV/T system. Goel et al. [32] looked at a variety of applications of nanofluid-based direct absorption solar collectors. Goel et al. [32] furnished future views on the challenges and developments faced by nanofluids as direct absorbers in hybrid PV/T applications. Xu and Kleinstreuer [33] proposed the use of a single-phase model of a CPV cooling system based on Al<sub>2</sub>O<sub>3</sub>/water nanofluid. The findings revealed that nanofluids considerably enhanced the electrical and overall efficiency of the investigated system. Another investigation was presented by DeJarnette et al. [34], who measured the spectral performance of a CPV-based nanofluids system employing silica-coated, Au nanorods, and indium tin oxide (ITO) nanocrystals, as well as a combination of ITO, CuSe, and Au nanorods as nanoparticles. The alternatives have been shown to provide good absorption and propagation performance for GaAs batteries.

Lately, Selim et al. [35] arranged Ag-SiO<sub>2</sub> center shell bunches employing an adjusted Stober technique including an alkali

**Table 1**  
Comparison between cooling techniques.

PV cooling method		Advantages	Disadvantages
<b>Passive cooling</b>	Heat-sink	<ul style="list-style-type: none"> <li>- Require additional energy.</li> <li>- Ease of manufacture and installation.</li> <li>- Flexibility in the placement of solar cells.</li> <li>- Enhanced the performance of PV under natural convection</li> </ul> <p><b>Lifetime:</b> Longer life</p>	<ul style="list-style-type: none"> <li>- Low efficiency compared to other techniques.</li> <li>- The turbulent airflow makes the heat sinks unstable.</li> <li>- The waste heat could be used for utilization</li> </ul>
	Transparent coating	<ul style="list-style-type: none"> <li>- PV cell temperature reduced drastically.</li> <li>- No space requirement needed.</li> <li>- Economical solution.</li> </ul> <p><b>Lifetime:</b> Long</p>	<ul style="list-style-type: none"> <li>- Heat reflected into space is wasted and might be used for domestic purposes instead.</li> </ul>
	PCM	<ul style="list-style-type: none"> <li>- Capable of storing large amounts of heat in response to modest temperature changes.</li> <li>- At a constant temperature, phase change occurs.</li> <li>- Absorbed heat can be exploited to heat the buildings.</li> </ul> <p><b>Lifetime:</b> Long</p>	<ul style="list-style-type: none"> <li>- In its solid state, paraffin has a limited heat conductivity.</li> <li>- Segregation reduces the total active volume for heat storage.</li> <li>- Less effective in cooler climates.</li> <li>- long-term degradation reactions with other materials</li> </ul>
<b>Active cooling</b>	Water immersion	<ul style="list-style-type: none"> <li>- Extremely effective.</li> <li>- Financial.</li> <li>- On clear days, electrical efficiency improved.</li> <li>- Safe for the environment.</li> </ul> <p><b>Lifetime:</b> Low due to ionized water reduces electrical efficiency.</p>	<ul style="list-style-type: none"> <li>- On cloudy and rainy days, efficiency is reduced.</li> <li>- The depth of submersion affects efficiency.</li> </ul>
	Forced air circulation	<ul style="list-style-type: none"> <li>- It is financially viable.</li> <li>- Overall efficiency has improved.</li> <li>- Heated air may be utilized to heat houses.</li> </ul> <p><b>Lifetime:</b> Low due to corrosion of PV panel.</p>	<ul style="list-style-type: none"> <li>- The efficiency of cooling with air is lower than that of cooling with water.</li> <li>- Water cooling is more beneficial than air cooling in hot weather.</li> </ul>
	Optical liquid filters	<ul style="list-style-type: none"> <li>- Use a liquid as the optical filter between sunlight and solar cell.</li> <li>- Significantly enhance PVT system performance.</li> <li>- The filters deliver only useable spectrum to the PV cells while others are filtered out.</li> </ul> <p><b>Lifetime:</b> Longer life</p>	<ul style="list-style-type: none"> <li>- The optical filter systems exhibited some good results, but very limited studies are available.</li> <li>- Nanofluid filters are expensive.</li> </ul>

catalyzed response. In all cases, the transmission electron microscope (TEM) review of the pre-arranged Ag–SiO<sub>2</sub> groups illustrates that nanoparticles can enhance total performance. Lee et al. [36] blended Ag–SiO<sub>2</sub> and Au–SiO<sub>2</sub> center shell nanoparticles through an analogous approach. James Walsheet et al. [37] created a variety of luminous imidzo-phenanthroline-based nanofluid filters for photovoltaic spectrum beam splitting. According to the nanofluid properties, the economic benefit of the acquired energy is boosted by up to 61% as compared to the host base fluid alone. As a result, the organic molecules included may be successfully constructed as high-performance, spectrally selective fluids for PVT applications.

The preceding studies showed that various experiments and numerical studies were conducted to test the effect of placing a liquid filter above the PV module under various conditions. Some of these systems use a specific thickness of the fluid layer, a specific material for the fluid container, and outdoor weather conditions. Table 1 provides a comparison between the different cooling techniques discussed previously. The comparison is based on the advantages, disadvantages, and lifetime of each cooling technique.

From this literature survey, even with plentiful studies and publications on the use of water or nanofluids in photovoltaic cooling applications. However, there are a limited number of studies associated with the shape of the filter and the exploitation of nanofluids as an optical filter in the cooling of CPVS concentrator photovoltaic systems. Besides, this paper is a numerical study done at the laboratory scale for non-commercial models. In addition, in the majority of experimental studies, the considered radiation is an artificial one, so the spectral distribution is not the same and the proposed results are permanent. Therefore, the novelty of this study is to look into the performance of a CPVS cooling system with optical filters and to put forward numerical relations. Also, the aim of the article is to predict the module's electrical, thermal, and overall efficiencies as functions of the investigated parameters.

The main objective of this paper, is to study three different shapes of optical water filter models. So, the thermal and electrical performance of the concentrator photovoltaic system CPVS with and without the optical water filter were determined under controlled weather conditions that have been validated before. Furthermore, the article proposes to investigate different water based nanofluid filter combinations (water-Al<sub>2</sub>O<sub>3</sub>, water-Cu, water-Ag, and water-Au). This investigation aims to study the system behavior to figure out the optimal nanofluid filter.

## 2. Methodology

### 2.1. System description practical

To validate the CFD model, the photovoltaic efficiency of the CPVS is compared to the experimental data previously carried out in our research laboratory by M. Chaabane et al. [38]. The experimental investigations were performed throughout the month of May in the Tunisian Saharan climate. Starting at 6:00 a.m., ng at 6 a.m., the PV cell temperature and photovoltaic efficiency measurement values were continuously monitored every 1/2 h.

The considered system, as illustrated in Fig. 2, is an ordinary concentration photovoltaic system (CPVS). It is composed of a concentrator and a photovoltaic panel. In order to acquire credible numerical validation results when modeling, one must focus on available correlations and equations and choose the most appropriate ones to apply for the various properties of the fluids and materials. These parameters are essential to know when solving the governing conservation equations. These properties mainly relate to thermal conductivity, viscosity, density, and heat capacity, on which the governing equations depend.

### 2.2. Mesh generation

The mesh generated in the entire field of this system, which is presented in Fig. 3, consists of hexahedral cells. A grid independence study was also carried out and the optimum mesh size was obtained with 960864 cells. Once the configuration is defined and meshed using Workbench, it has been exported to ANSYS 16.0 for the numerical simulation.

### 2.3. Assumptions

The assumptions considered in the calculation domain are listed below:

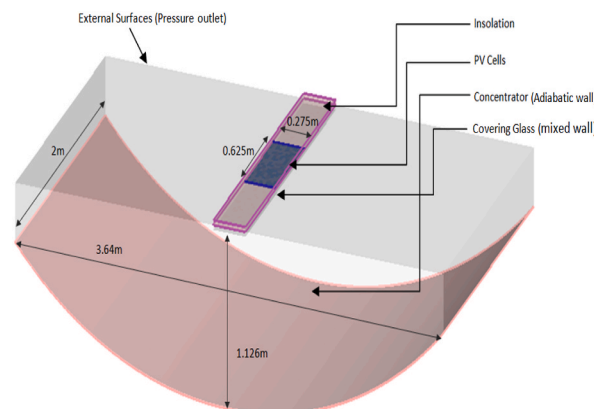


Fig. 2. Description of CPVS and associated boundary conditions.



Fig. 3. The generated grid for the CPVS system.

- Incompressible fluid.
- Boussinesq approximation is assumed to be valid for air, within the range of temperatures considered. The thermal properties of the air are constant, except for the air's density which varies linearly with temperature according to the Boussinesq approximation:

$$(\rho - \rho_{air}) = \rho_{air}\beta (T - T_{r,air}) \tag{1}$$

With:  $\rho_{air}$  is the air density at the reference temperature  $T_{r, air}$ .  
 $\beta$  is the thermal expansion coefficient of the air.

- The dirt and dust on the PV cell's glass and the reflector are negligible.
- The whole system is initially assumed to be at the defined initial ambient temperature  $T_{amb}$ .

2.4. Governing equations

The Navier-Stokes conservation equations for a three-dimensional turbulent flow are considered taking into account the Boussinesq hypothesis. For the closure of these equations, the standard K-ε turbulence model has been considered which allows a fast calculation time and a good prediction for such flow [39]. Five radiation models are available in ANSYS fluent software, but only the discrete ordinate (DO) model is suitable for a selective material such as the photovoltaic cells. For that, the (DO) model was chosen as it allows also to specify different values for the absorption coefficient and the reflection index in the materials panel for each one of the spectrum bands previously defined. The governing equations of continuity, momentum, energy, turbulence, and radiation are provided in Table 2.

2.5. Boundary conditions

For the climatic conditions, global irradiance and ambient temperature are taken from the experiments and introduced as inputs for CFD simulations. These parameters are taken from the experiments which have been conducted in a Tunisian Saharan climate, in the city of Tozeur, on the 31<sup>st</sup> of May. The external sky temperature  $T_{sky}$  required for estimating the radiation exchange is introduced as a

Table 2  
 Summary of the governing equations.

the governing equations of mass, momentum, and energy Equations	The continuity equation: $\frac{\partial \rho}{\partial t} + \text{div}(\rho v) = 0$ (2)	$\rho$ fluid density $v$ vector of velocity
	The momentum conservation equation: $\frac{\partial(\rho v)}{\partial t} + \nabla \cdot (\rho v v) = -\nabla P + \nabla \cdot \bar{\tau} + \rho \cdot g + F$ (3)	P static pressure $\bar{\tau}$ stress tensor E energy transfer term
	The energy conservation equation: $\frac{\partial(\rho E)}{\partial t} + \nabla \cdot (v(\rho E + P)) = \nabla \cdot (K_{eff} \nabla T - \sum_j h_j J_j + (\bar{\tau}_{eff} \cdot v)) + S_h$ (4)	$K_{eff}$ effective conductivity F external body force $h_j$ the enthalpy of the species j $\bar{\tau}_{eff}$ viscous stress tensor $S_h$ volumetric heat source $J_j$ diffusion flux of the species j.
Turbulence equations	$\frac{\partial}{\partial t}(\rho k) + \frac{\partial}{\partial x_i}(\rho k \tilde{u}_i) = \frac{\partial}{\partial x_i} \left[ \left( \mu + \frac{\mu_t}{\sigma_k} \right) \frac{\partial k}{\partial x_j} \right] + G_k + G_b - \rho \epsilon + Y_M + S_k$ (5)	$G_k$ generation of turbulence kinetic energy
	$\frac{\partial}{\partial t}(\rho \epsilon) + \frac{\partial}{\partial x_i}(\rho \epsilon \tilde{u}_i) = \frac{\partial}{\partial x_j} \left( \left( \mu + \frac{\mu_t}{\sigma_\epsilon} \right) \frac{\partial \epsilon}{\partial x_j} \right) + C_{1\epsilon} \frac{\epsilon}{k} (G_k + C_{3\epsilon} G_b) - C_{2\epsilon} \rho \frac{\epsilon^2}{k} + S_\epsilon$ (6)	$G_b$ generation of turbulence kinetic energy due to buoyancy
	$\mu_t = C_\mu \frac{k^2}{\epsilon}$ (7)	$Y_M$ contribution of fluctuating dilatation incompressible turbulence to the overall dissipation rate. $S_k$ and $S_\epsilon$ are the source terms. $\mu_t$ is the turbulence viscosity $C_\mu, C_{1\epsilon}, C_{2\epsilon}, C_{3\epsilon}$ Empirical constants of the standard k - ε model
The DO radiation Model Equation	$\frac{dI(\vec{r}, \vec{s})}{ds} = -(a + \sigma_s)I(\vec{r}, \vec{s}) + a \left( \frac{\sigma T^4}{\pi} \right) + \frac{\sigma_s}{4\pi} \int_0^{4\pi} I(\vec{r}, \vec{s}') \Phi(\vec{s}, \vec{s}') d\Omega'$ (8)	The DO model considers the radiative transfer equation RTE in the direction $\vec{s}$ as a field equation. $\lambda$ wavelength $a_s$ spectral absorption coefficient.

user-defined function UDF. It is expressed as follows, according to the change in ambient temperature:

$$T_{\text{sky}} = 0.0552 T_{\text{amb}}^{1.5} \quad (9)$$

The CPVS was south facing and  $34^\circ$  titled above the horizontal. The system description and the attributed boundary conditions are illustrated in Fig. 2. The boundary conditions considered for the different components of the solar system are:

- The concentrator is defined as an adiabatic wall: heat flux =  $0 \text{ w/m}^2$  (it is totally reflective)
- The PV cells are defined as coupled which allows introducing all the heat transfer modes in this surface.
- The glass covering the PV cells is defined as mixed in order to take into account the convection and radiation heat transfer at this surface.
- The external covering surface is defined as a pressure outlet.

Based on the CFD simulation results; it was possible to have the temperature of the photovoltaic cells and to calculate the numerical efficiency using the photovoltaic efficiency formula defined by Dubey et al. [40]. Equation (10) represents the traditional linear expression for photovoltaic efficiency.

$$\eta_{\text{pv}} = \eta_{\text{Tref}} [1 - \beta_{\text{ref}} (T_{\text{pv}} - T_{\text{ref}})] \quad (10)$$

With:  $\eta_{\text{pv}}$  = photovoltaic efficiency.

The  $T_{\text{ref}}$  = reference temperature at the standard temperature condition STC, which is defined for solar radiation of  $1000 \text{ W/m}^2$ ,  $T_{\text{ref}} = 25^\circ\text{C}$ ,  $\eta_{\text{ref}}$  = photovoltaic performance at  $T_{\text{ref}}$ ,  $\eta_{\text{Tref}}$  and  $\beta_{\text{ref}}$  are normally given by the PV manufacturer.  $\beta_{\text{ref}}$  depends not only on the PV material but also on  $T_{\text{ref}}$ , as well. It is given by the ratio:

$$\beta_{\text{ref}} = 1 / (T_0 - T_{\text{ref}}) \quad (11)$$

In which  $T_0$  is the temperature at which the electrical performance of the module falls to zero. For monocrystalline silicon, this temperature is chosen as  $T_0 = 270^\circ\text{C}$ .

## 2.6. Numerical procedures

The given governing equations are solved by the finite volume method in the unsteady regime. The energy equation was selected as a heat transfer model. To solve the mean flow equations, the standard k- $\epsilon$  model was used as a computational method. Besides, the radiation model DO was selected not only because it's suitable for the selected material, like that of the photovoltaic cells, but also because it is accurate and has a short computation time.

As for the precision of the result, the terms of continuity, velocity, and turbulence are solved by the convergence criteria of  $10^{-4}$ , while a value of  $10^{-6}$  is imposed for energy. A 2nd order upwind scheme is chosen to discretize velocity, turbulent kinetic energy, turbulent dissipation rate, and energy, while the Presto scheme is chosen for the pressure discretization. The problem is now ready to be iterated as all the necessary input conditions have been set.

## 3. Numerical results

### 3.1. Numerical model validation

To examine the accuracy of the proposed model, the numerical solution is validated with experimental data from M. Chaabane et al. [41] for a concentrator photovoltaic system (precise descriptions of the operating conditions can be found in M. Chaabane et al. [41]).

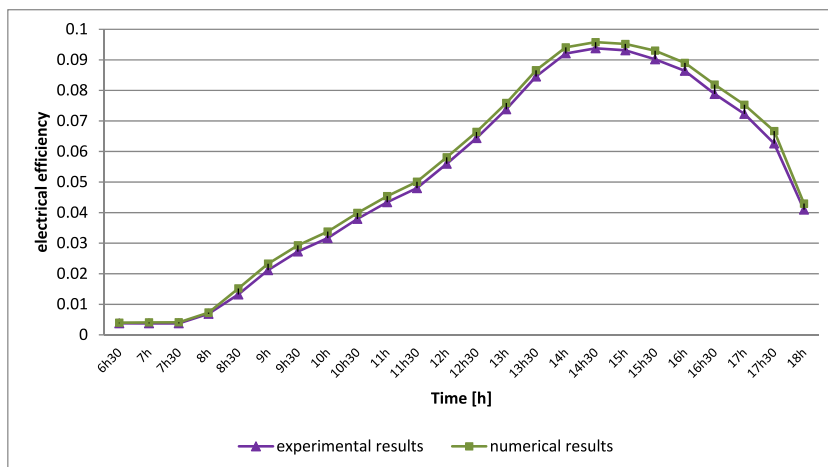


Fig. 4. Validation of numerical results with experiments of the temporal evolution of the electrical efficiency of the CPVS.

The reflector is considered opaque and non-selective with an absorptivity of  $\alpha = 0.05$ . The PV glass is a transparent wall with the following optical properties, an absorptivity  $\alpha = 0.02$  and a transmissivity  $\tau = 0.95$ .

Fig. 4 shows the numerical photovoltaic efficiency compared favorably with the experimental data, with an average error of less than 2%. It can be concluded that the proposed CFD model of the CPVS has acceptable accuracy in the numerical solution. For the following part of this article, The CPVS is equipped with an optical water filter as a PV cooling method. Three different shapes of OWF are investigated and compared to the base case model.

### 3.2. Effect of optical water filter OWF use

In this section, the effect of the addition of an optical water OWF filter on the CPVS is investigated for different OWF models. This study aims to evaluate the performance of CPVS for three different OWF models. As described in Fig. 5, the modeled optical water filter OWF consists of a glass tank with a cover having the same length and width as the PV module. The tank and cover are made of glass with a 3 mm thickness and 91% transmittance. In this system, the solar spectrum passes over the water filter, which acts as a spectrum window, and consequently, the incident radiation is split to meet the spectral response of crystalline silicon solar cells.

In order to discuss the effects of the addition of different optical water filters on the validated basic system, changes in the shape of the filter are concerned, as shown in Fig. 6, and three different models of optical water filters have been used. In model (I), an optical water filter was placed just below the photovoltaic cells. In model (II), the water passes over and under the photovoltaic cells with separate inputs. Model (III) is characterized by a double pass mode. All three models are studied under the climatic conditions of the Tunisian Sahara, and a comparative study is conducted to evaluate the electrical and thermal efficiency of the considered PV/T models. For the study of all these models, the same simulation models used for the numerical validation were considered. The inlet water velocity is fixed at 0.05 l/s.

The modeled optical water filter OWF consists of a glass tank with a cover having the same length and width as the PV module. The tank and cover are made of 3 mm thick glass and 91% transmission. The breadth of the water filter is 5 cm. The purpose of this section is to analyze the filter models described above and to evaluate their effects in terms of photovoltaic cell protection, which indeed helps to improve their electrical performance and also recover thermal energy. The three filter models studied are used as a cooling system to improve the electrical efficiency of the concentrated photovoltaic panel. Optical properties are important parameters that affect the filters operating. The two most significant optical properties that generally evaluate the optical performance of filters are the transmittance and the absorbance.

From that point, using a non-gray radiation model like the DO, the “Gray-Band Absorption Coefficient” and the “Gray-Band Reflection Index” allow us to indicate alternate assimilation of the absorption coefficient and the reflection index on the materials board for each band pecified in the radiation section. In this paper, both the absorption coefficient and the reflection index of the water are characterized with the assistance of values given by Hale et al. [42], Buiteveld et al. [43], and Himanshu et al. [44].

Fig. 7 compares the electrical efficiency of the photovoltaic system without an optical filter and with the selected filter models. It is shown that the photovoltaic efficiency rises from 6:30 to 13:00, remains relatively stable between 13:00 and 15:00, and drops from 14:00 to 18:00. It's notable that the double-pass optical filter model (III) can achieve the highest photovoltaic efficiency, and its photovoltaic efficiency has the smallest range of variation compared to other cooling modes throughout the day. This difference is due to the coupling between two heat transfer modes: the forced convection for the upper part of the passage and the radiance applied to the optical filter below the photovoltaic cells. The figure also shows the effect of circulating water for the filter models studied on the daily variation of the electrical output provided by the CPVTS. It's noteworthy that the exhibitions of the CPVS are upgraded with the optical spectrum filter because of the evasion of the adverse consequence of temperature increase on PV cells. Indeed, the maximum electrical efficiency achieved by the basic CPVTS is about 9.7%, while that corresponding to the systems with filters I, II, and III is respectively 10.51%, 11.6%, and 12.08%. This rise in electrical efficiency, with the use of the OWF, is due to the reduction of the negative effect of the PV temperature on the system efficiency. This system also presents the advantage of a significant thermal production.

So, in addition to controlling the electrical efficiency to assess this contribution, the water outlet temperatures were also tempered for the studied models. These results are illustrated in Fig. 8, which shows that the output temperature, which reaches 54 °C, is higher in the water filter model (III), which was also associated with the maximum electrical performance. This is beneficial as PV's efficiency is reduced as PV temperature is increased. Indeed, the OWF is performing as a spectrum porthole that transmits the visible and a part of

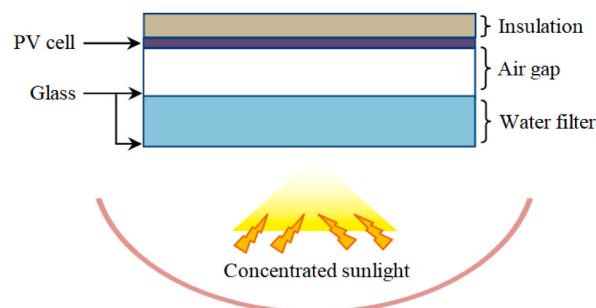


Fig. 5. Schematic of the water optical filter.

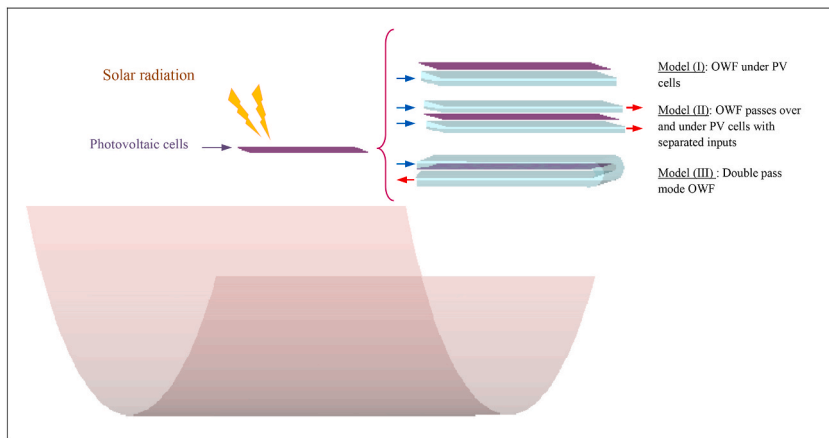


Fig. 6. The studied models of optical water filter water outflow.

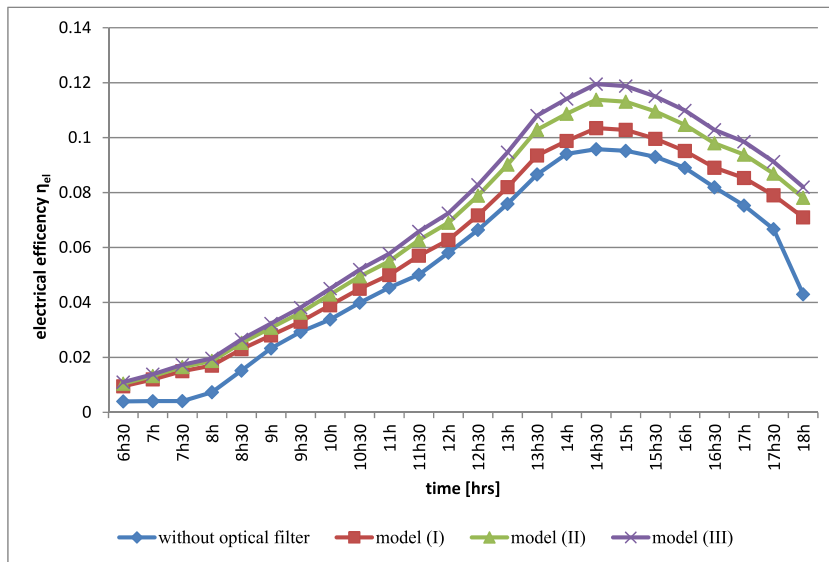


Fig. 7. Temporal evolution of the electrical efficiency of the CPVS.

the infrared radiation while filtering the ultraviolet and some of the infrared radiation, which is unaccustomed to the photovoltaic conversion of solar radiation. This explains this global system performance enhancement.

#### 4. Application of nanofluids in CPVS as an optical filter

It has already been shown in the previous part of this paper that the liquid filters can fractionate the spectral beam and absorb non-useful bands for photovoltaic conversion, which has an impact on the enhancement of the electrical efficiency in addition to the thermal production. To advance these hybrid systems, it is necessary to combine them with liquid filters capable of improving the combined conversion efficiency by controlling their thermal and optical characteristics.

Heat transfer fluids such as glycols, motor oil, and water are commonly utilized. Additionally, employing these classic fluids reduces the need for heat exchangers. It might be increased by including particles like nanofluid attachment materials or hanging substances into the base fluid, as well as enhancing heat conductivity in traditional fluids [45]. In general, nanoparticles have been shown to greatly boost the thermal conductivity of the base fluid [46]. The study that follows is centered on determining the effects of adding nanofluids to filter channels on the framework’s efficacy. Meanwhile, an analysis of the photovoltaic and thermal efficiency of the CPVS-nanofluid is provided to evaluate the nanofluid filter’s productivity.

Nanofluid is a novel type of fluid suspension made up of nanoscale (100 nm) particles that are uniformly dispersed and suspended in a base fluid. These fluid composites have attracted a lot of attention during the last decade compared to conventional fluids. This increase in the use of nanofluids is due to their heat absorption capacity and their optical properties for the division of the complete

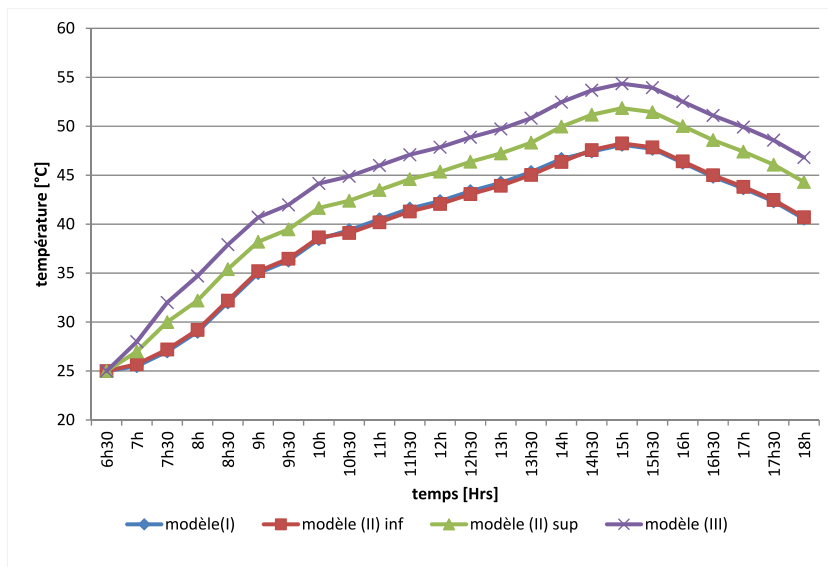


Fig. 8. Temporal evolution of water output temperature for different studied model.

solar spectrum (PV band and thermal bands). In this part, it is proposed to study the influence of the concentration of nanoparticles dispersed in a base fluid (water) on the electrical efficiency of the concentrated photovoltaic system studied in the previous part. To do this, the model (III) was adopted as it showed the best performance. By following a numerical procedure similar to the one considered in the previous section, the effect of the insertion of the nanofluid on the considered optical filter model is investigated.

To get solid numerical results when modeling, accessible correlations are considered to pick the most appropriate one to apply for the different properties of a nanofluid [47]. These properties may incorporate thermal conductivity, viscosity, density, and heat capacitance depending on what form the governing equations are written. Similar to any fluid mechanics and heat transfer problem based on the resolution of the main conservation equations of flow, the numerical study of nanofluids with specific geometric shapes can be carried out. When solving, CFD codes are based on the same governing equations described in the previous part of this article, in addition to two-phase modeling. The multiphase mixture model allows the coupling between two or more non-miscible fluids by solving the governing equations for the mixture and the volume fraction equations for the secondary phases. Typical applications of this model include the transient motion of a liquid-gas, liquid-liquid, or liquid-particle mixture.

The mixture model is a method based on the notion of the volume fraction. This notion of volume fraction, denoted  $\alpha$ , represents the rate of presence of one of the fluids in each control volume. It varies between 0 and 1 for the phase under consideration. Let's say a phase p and a phase q:

- $\alpha = 0$ ; only phase p is present in the control volume.
- $\alpha = 1$ ; only phase q is present in the control volume.
- the volume contains both phases at once.

The follow-up of the mixture is carried out by solving the continuity equation for the density fraction  $\alpha_q$  for a phase q:

$$\frac{\partial}{\partial t} (\alpha_q \rho_q) + \left( \nabla \cdot (\alpha_q \rho_q \vec{v}_q) \right) = 0 \tag{12}$$

The nanofluid optical filter applied to the CPVS ought to change the sunlight-based lighting to transmit all photons inside the PV spectral response bandwidth and retain different photons outside this interval. In such a manner, examining the thermal characteristics and optical properties (absorption coefficient and reflection index) of the selected nanofluids and their effect on the productivity of the CPVS system is viewed as a significant piece of this study. For the modeling of the nanofluid, the same boundary conditions described above were considered, and the multiphase model "Mixture" with two phases was activated. The first of which is the base fluid "water"

Table 3  
Thermodynamic and optical properties of the selected nanoparticles.

	Density ( $\rho$ ) [kg. m <sup>-3</sup> ]	Specific heat (Cp) [kJ. kg <sup>-1</sup> K <sup>-1</sup> ]	Thermal conductivity ( $\lambda$ ) [W. m <sup>-1</sup> K <sup>-1</sup> ]	Optical properties
Water	997.1	4179	0.613	[42,43]
Al <sub>2</sub> O <sub>3</sub>	3970	765	40	[48]
Cu	8960	385	401	[49]
Ag	10500	235	429	[50,51]
Au	19320	129	318	[52,53]

and the second is the nanofluid. The numerical analysis was done using nanofluid for optical filtration through nanoparticles with a volume fraction density  $\alpha_f = 2\%$ , a diameter of 5 nm, and the same speed as water at 0.05 l/s. Many considerations were taken to evaluate the CPVS's performance, like temperature gain through the nanofluid as well as electrical and thermal efficiencies. Table 3 summarizes the thermodynamic and optical properties of each selected nanoparticle.

The performance of the considered system was evaluated under a wide variety of nanofluid water-based filters. In Fig. 9, the variation of the photovoltaic efficiency of the CPVS at different nanofluids is depicted. It can be seen that the photovoltaic efficiency fluctuates widely when altering the different selected fluid filters with nanofluid. The main reason behind this is that the photovoltaic efficiency enhancement is a result of the optical filtration, which boosts the solar obstruction and adversely impacts the electric output of the CPVS conversion process. This is due to the tradeoff between illumination absorption in the lower filter and heat absorption in the upper flow channel owing to heat dissipation to the filter and higher heat loss. This leads to a decrease in the heat transfer rate between the filter and the PV, which in turn, leads to a decrease in the operating temperature of the PV cells. It can also be noticed that the optimal thermal efficiency of the system is achieved by the water-Au filter on account of the enhancement of solar radiation absorption rate, and the corresponding variation in the electrical efficiency is between 2% and 18%.

Similarly, the outlet temperature of the nanofluid filter is illustrated in Fig. 10. Results show that using a nanofluid as an optical spectrum filter, compared with the water filter, uniquely enhances the outlet temperature of 2.9 °C, 4.5 °C, 8.2 °C, and 11.1 °C for water-Al<sub>2</sub>O<sub>3</sub>, water-Cu, water-Ag, and water-Au filters, respectively. This temperature improvement is attributable to an increase in the heat transfer coefficient due to the inclusion of nanoparticles in the optical filter. This makes it easier to have lower PV cells' temperature for better photovoltaic efficiency and ensures better reuse of filter fluid for domestic or industrial recognizable customs. From the results shown in Figs. 9 and 10, it could be concluded that the optimal photovoltaic efficiency is attempted for high solar radiation (from 12 h30). Indeed, the nanofluid filter plays the role of a spectrum window that absorbs the waves of the unwanted thermal wavelengths (outside the photovoltaic spectrum), transforms them into heat ready for use, and facilitates the cells' temperature reduction in their turn.

In addition to the electrical considerations, the water outlet temperature was also measured in order to evaluate the system's thermal efficiency. The thermal efficiency of the CPVS is illustrated for the considered water mass flow rates in the major advantage of water optical filters, which is the protection of photovoltaic cells from unwanted frequencies in addition to its thermal production. The thermal efficiency of the various studied nanofluid filters is calculated and plotted in Fig. 11, according to the ratio  $\Delta T/G$ , which links the increase in the water temperature to the solar flux G. An expected behavior for the increasing of the thermal efficiencies of all studied cases is shown. It has also been noticed that the thermal efficiency decreases linearly with the variable  $\Delta T/G$ . The thermal efficiency of such a device is given by the following expression [54]:

$$\eta_{th} = F' \left( \eta_0 - U_c \frac{A_b}{A_c} \frac{\Delta T}{G} \right) \tag{13}$$

The overall coefficient of thermal losses  $U_c$  is determined from the slope of the instantaneous thermal yield curve given by  $U_c F' \frac{A_b}{A_c}$

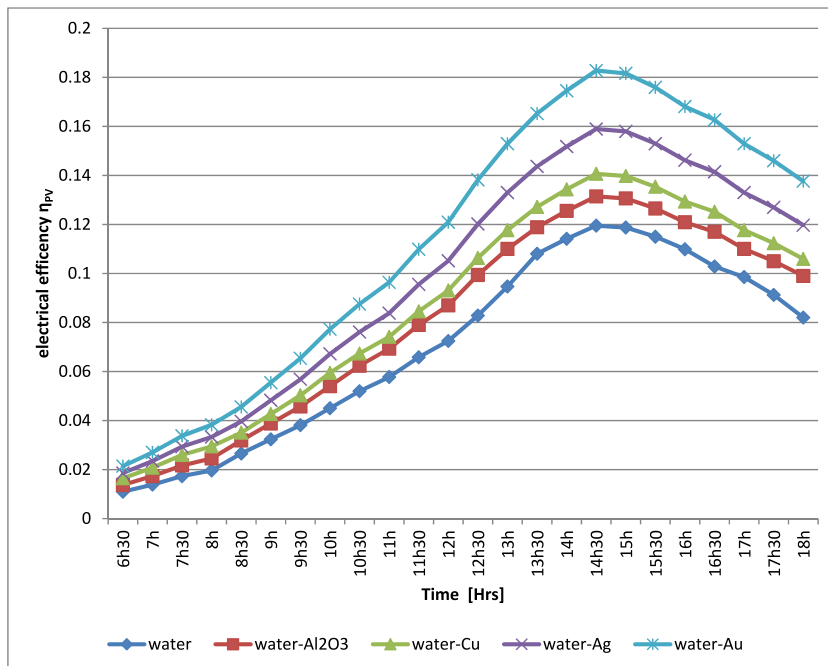


Fig. 9. The variance in photovoltaic efficiency of the CPVS with different nanofluids.

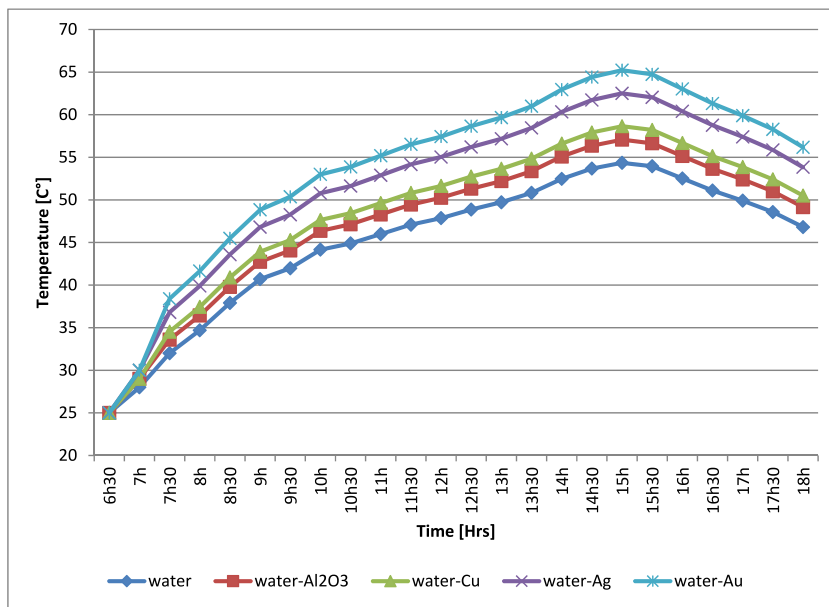


Fig. 10. The temporal evolution of water output temperature for different nanofluid.

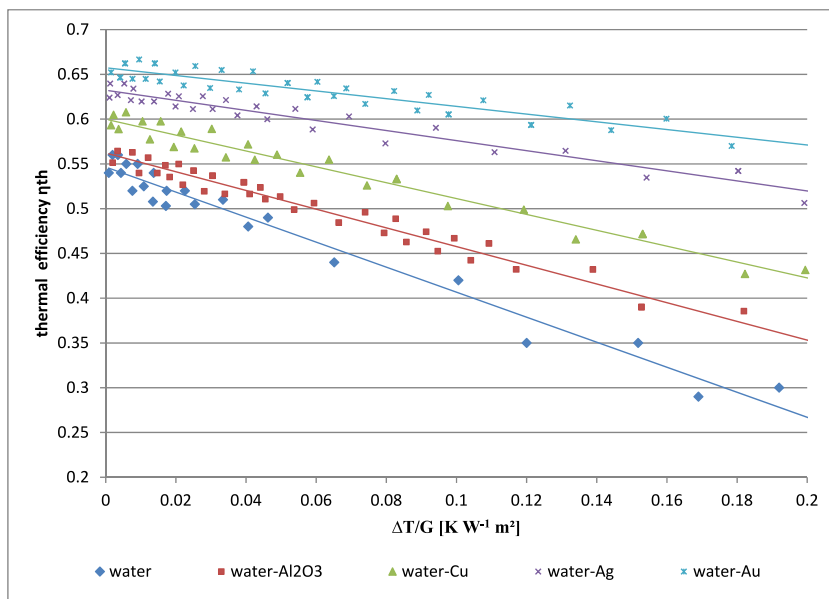


Fig. 11. Evolution of the thermal efficiency for the different nanofluid.

and originating  $F'\eta_0$ . These systems' efficiency factors and overall coefficient of heat loss are given in Table 4.

Based on the values presented in Table 4, the addition of nanofluid filters to photovoltaic cells improves the thermal efficiency of the concentrator. However, it causes an increase in overall heat losses to the external environment. Regarding the efficiency factor of the sensor, it remains almost invariant and very close to 1. This result is very predictable because the filter is thin and it is a good heat conductor. This is mainly due to their particular thermo-physical properties like their high thermal conductivity, which is an essential criterion for heat transfer enhancement as well as their important specific heat.

### 5. Conclusion

This paper is a numerical investigation using CFD tools into the performance of a concentrator photovoltaic system based on liquid absorption spectral beam filters. Based on our experimental data and after the model validation, three different optical filter structure models have been developed. The effects of the optical filter shape on the systems' electrical and thermal performances are analyzed. In

**Table 4**

Overall loss coefficient and efficiency factor of the concentrated photovoltaic sensor with different studied nanofluid filters.

	Water	Water-Al <sub>2</sub> O <sub>3</sub>	Water-Cu	Water-Ag	Water-Au
U <sub>c</sub>	48.2	50.1	51.6	53.8	55.7
F'	0.93604	0.95618	0.96625	0.97813	0.98552

the current study, in order to improve the performance of the CPVS with an optical water filter, the addition of different nanofluids as an optical filter is also proposed. The most important conclusions that can be drawn from this paper are as below:

- The article pointed out different effects associated with the use of OWF optical water filters of different models. The results showed a significant increase in the outlet water temperature, reaching 54 °C for the water filter model (III), which is also associated with maximum electrical performance.

- The maximum photovoltaic efficiency achieved by the basic CPVTS is approximately 9.7%, while that corresponding to the systems with filter models I, II, and III are respectively 10.51%, 11.6%, and 12.08%. According to the performance analysis of the PV system, the use of OWF was thus found to be extremely beneficial as it resulted in an increase in electrical efficiency.

- The addition of nanoparticles, with a volume fraction density fraction of  $\alpha_f = 2\%$ , a diameter of 5 nm, and the same speed as the water (0.05 l/s), enhances the photovoltaic efficiency by up to 10%.

- Investigations of different water-based nanofluid combinations (water-Al<sub>2</sub>O<sub>3</sub>, water-Cu, water-Ag, and water-Au) were proposed. The nanofluid filters upgrade the CPVS performance not only owing to their thermodynamic properties but also as beam splitters. Compared to the reference case (optical water filter without nanoparticles), the best performance was obtained by using a water-Au nanofluid optical filter.

This work has demonstrated that optical nanofluid filters can enhance PV/T system's performance, resulting in hybrid solar systems with higher thermal and photovoltaic efficiencies than alternatives based on standard PV/T systems that do not use spectral splitting principles.

The most important limitation of this study is that it is a comparison of different nanofluid filters with different thermodynamic and optical properties. An examination should be conducted to focus on the understanding of the influence these properties have on PV system efficiencies. For further studies, a comprehensive method for identifying the appropriate and optimal liquid filters for each type of photovoltaic cell should be proposed. Also, determining the efficiency limitations of spectrum splitting for photovoltaic cooling systems would have to be done. As an optical filter depends on the type of liquid filter, the nature of the PV cells, and the PV/T applications, the objective is, therefore, to identify the ideal filter for a spectrum-separated PV/T cooling system.

#### Authors statement

A. Jannen devised the conceptual ideas, including writing, reviewing, designing the model, computational framework, data analysis, and draft preparation. M. Chaabane verified the analytical methods and investigation. H. Mhiri and P. Bournot performed the visualization, funding acquisition and supervised the findings of this work. All persons who meet authorship criteria are listed as authors, and all authors certify that they have participated sufficiently in the work to take public responsibility for the content, including participation in the concept, design, analysis, writing, or revision of the manuscript. Furthermore, each author certifies that this material or similar material has not been and will not be submitted to or published in any other publication before its appearance in the Case Studies in Thermal Engineering Journal.

#### Declaration of competing interest

The authors declare that they have no known competing financial interests or personal relationships that could have appeared to influence the work reported in this paper.

#### References

- [1] S. Kumar, M.K. Rawat, S. Gupta, An evaluation of current status of renewable energy sources in India, *Int. J. Innovative Technol. Explor. Eng.* 8 (10) (2019) 1234–1239, <https://doi.org/10.35940/ijitee.G6004.0881019>.
- [2] A.M. Elbreki, et al., The role of climatic-design-operational parameters on combined PV/T collector performance: a critical review, *Renew. Sustain. Energy Rev.* 57 (2016) 602–647, <https://doi.org/10.1016/j.rser.2015.11.077>.
- [3] R.A. Taylor, T. Otanicar, G. Rosengarten, Nanofluid-based optical filter optimization for PV/T systems, *Light Sci. Appl.* 1 (2012) 1–7, <https://doi.org/10.1038/lsa.2012.34>. OCTOBER.
- [4] L. Zhu, R.F. Boehm, Y. Wang, C. Halford, Y. Sun, Water immersion cooling of PV cells in a high concentration system, *Sol. Energy Mater. Sol. Cells.* 95 (2) (2011) 538–545, <https://doi.org/10.1016/j.solmat.2010.08.037>.
- [5] F. Yazdanifard, M. Ameri, Exergetic advancement of photovoltaic/thermal systems (PV/T): a review, *Renew. Sustain. Energy Rev.* 97 (August) (2018) 529–553, <https://doi.org/10.1016/j.rser.2018.08.053>.
- [6] S.M. Salih, O.I. Abd, K.W. Abid, Performance enhancement of PV array based on water spraying technique, *International Journal of Sustainable and Green Energy*, February (2015), <https://doi.org/10.11648/j.ijrse.s.2015040301.12>.
- [7] J. Siecker, K. Kusakana, B.P. Numbi, A review of solar photovoltaic systems cooling technologies, *Renew. Sustain. Energy Rev.* 79 (2017) 192–203, <https://doi.org/10.1016/j.rser.2017.05.053>. July 2016.
- [8] T.P. Otanicar, I. Chowdhury, R. Prasher, P.E. Phelan, Band-gap tuned direct absorption for hybrid concentrating solar photovoltaic/thermal system, in: *ASME/JSM E 2011 8th Thermal Engineering Joint Conference*, AJTEC 2011 133, 2011, pp. 1–7, <https://doi.org/10.1115/1.4004708>. November 2011.
- [9] E.Z. Ahmad, A. Fazlizan, H. Jarimi, K. Sopian, A. Ibrahim, Enhanced heat dissipation of truncated multi-level fin heat sink (MLFHS) in case of natural convection for photovoltaic cooling, *Case Stud. Therm. Eng.* 28 (2021), 101578, <https://doi.org/10.1016/j.csite.2021.101578>. March.

- [10] T.M. Sathe, A.S. Dhole, A review on recent advancements in photovoltaic thermal techniques, *Renew. Sustain. Energy Rev.* 76 (2017) 645–672, <https://doi.org/10.1016/j.rser.2017.03.075>. March.
- [11] M. Chaabane, H. Mhiri, P. Bournot, Effect of the storage tank thermal insulation on the thermal performance of an integrated collector storage solar water heater (ICSSWH), *Heat Mass Tran.* 50 (10) (2014) 1335–1341, <https://doi.org/10.1007/s00231-014-1345-x>.
- [12] S.S. Chandel, T. Agarwal, Review of cooling techniques using phase change materials for enhancing efficiency of photovoltaic power systems, *Renew. Sustain. Energy Rev.* 73 (2017) 1342–1351, <https://doi.org/10.1016/j.rser.2017.02.001>. October 2016.
- [13] F. Hachem, B. Abdulhay, M. Ramadan, H. El Hage, M.G. El Rab, M. Khaled, Improving the performance of photovoltaic cells using pure and combined phase change materials – experiments and transient energy balance, *Renew. Energy* 107 (2017) 567–575, <https://doi.org/10.1016/j.renene.2017.02.032>.
- [14] A. Karthick, P. Ramanan, A. Ghosh, B. Stalin, R. Vignesh Kumar, I. Baranilingesan, Performance enhancement of copper indium diselenide photovoltaic module using inorganic phase change material, *Asia Pac. J. Chem. Eng.* 15 (5) (2020) 1–11, <https://doi.org/10.1002/apj.2480>.
- [15] D.K. Rao, K.S. Reddy, V.V.S. Rao, PVT cell performance characteristics and efficiency with phase change material, *Int. J. Eng. Adv. Technol.* 9 (5) (2020) 1005–1012, <https://doi.org/10.35940/ijeat.e1053.069520>.
- [16] S.A. Memon, Phase change materials integrated in building walls: a state of the art review, *Renew. Sustain. Energy Rev.* 31 (2014) 870–906, <https://doi.org/10.1016/j.rser.2013.12.042>.
- [17] H.G. Teo, P.S. Lee, M.N.A. Hawlader, An active cooling system for photovoltaic modules, *Appl. Energy* 90 (1) (2012) 309–315, <https://doi.org/10.1016/j.apenergy.2011.01.017>.
- [18] J.K. Tonui, Y. Tripanagnostopoulos, Air-cooled PV/T solar collectors with low cost performance improvements, *Sol. Energy* 81 (4) (2007) 498–511, <https://doi.org/10.1016/j.solener.2006.08.002>.
- [19] X. Han, Y. Wang, L. Zhu, Electrical and thermal performance of silicon concentrator solar cells immersed in dielectric liquids, *Appl. Energy* 88 (12) (2011) 4481–4489, <https://doi.org/10.1016/j.apenergy.2011.05.037>.
- [20] P. Dwivedi, K. Sudhakar, A. Soni, E. Solomin, I. Kirpichnikova, Advanced cooling techniques of P.V. modules: a state of art, *Case Stud. Therm. Eng.* 21 (May) (2020), 100674, <https://doi.org/10.1016/j.csite.2020.100674>.
- [21] S.R. Reddy, M.A. Ebadian, C.X. Lin, A review of PV-T systems: thermal management and efficiency with single phase cooling, *Int. J. Heat Mass Tran.* 91 (2015) 861–871, <https://doi.org/10.1016/j.ijheatmasstransfer.2015.07.134>.
- [22] X. Han, X. Zhao, J. Huang, and J. Qu, “Optical properties optimization of plasmonic nanofluid to enhance the performance of spectral splitting photovoltaic/thermal systems,” *Renew. Energy*, vol. 188, pp. 573–587, Apr. 2022, doi: 10.1016/j.renene.2022.02.046.
- [23] A. S. Abdelrazik, F. A. Al-Sulaiman, and R. Saidur, “Feasibility study for the integration of optical filtration and nano-enhanced phase change materials to the conventional PV-based solar systems,” *Renew. Energy*, vol. 187, pp. 463–483, Mar. 2022, doi: 10.1016/j.renene.2022.01.095.
- [24] A. Qahtan, S.P. Rao, N. Keumala, The effectiveness of the sustainable flowing water film in improving the solar-optical properties of glazing in the tropics, *Energy Build.* 77 (2014) 247–255, <https://doi.org/10.1016/j.enbuild.2014.03.051>.
- [25] W.A.M. Al-Shohani, R. Al-Dadah, S. Mahmoud, Reducing the thermal load of a photovoltaic module through an optical water filter, *Appl. Therm. Eng.* 109 (2016) 475–486, <https://doi.org/10.1016/j.applthermaleng.2016.08.107>.
- [26] R. Looser, M. Vivar, V. Everett, Spectral characterisation and long-term performance analysis of various commercial Heat Transfer Fluids (HTF) as Direct-Absorption Filters for CPV-T beam-splitting applications, *Appl. Energy* 113 (2014) 1496–1511, <https://doi.org/10.1016/j.apenergy.2013.09.001>.
- [27] G. Wang, B. Wang, X. Yuan, J. Lin, Z. Chen, Novel design and analysis of a solar PVT system using LFR concentrator and nano-fluids optical filter, *Case Stud. Therm. Eng.* 27 (May) (2021), 101328, <https://doi.org/10.1016/j.csite.2021.101328>.
- [28] M.M. Abd El-Samie, W. Li, C. Xu, X. Ju, Influence of thermal and optical criteria of spectral fluid filters for hybrid concentrated photovoltaic/thermal systems, *Int. J. Heat Mass Tran.* 174 (2021), 121303, <https://doi.org/10.1016/j.ijheatmasstransfer.2021.121303>.
- [29] A.K. Alanazi, Y. Khetib, H.M. Abo-Dief, M. Rawa, G. Cheraghian, M. Sharifpur, The effect of nanoparticle shape on alumina/EG-water (50:50) nanofluids flow within a solar collector: entropy and exergy investigation, *Case Stud. Therm. Eng.* 28 (2021), 101510, <https://doi.org/10.1016/j.csite.2021.101510>.
- [30] A. Radwan, M. Ahmed, S. Ookawara, Performance enhancement of concentrated photovoltaic systems using a microchannel heat sink with nanofluids, *Energy Convers. Manag.* 119 (2016) 289–303, <https://doi.org/10.1016/j.enconman.2016.04.045>.
- [31] H.A. Kazem, A.H.A. Al-Waeli, M.T. Chaichan, K. Sopian, Numerical and experimental evaluation of nanofluids based photovoltaic/thermal systems in Oman: using silicone-carbide nanoparticles with water-ethylene glycol mixture, *Case Stud. Therm. Eng.* 26 (2021), 101009, <https://doi.org/10.1016/j.csite.2021.101009>. March.
- [32] N. Goel, R.A. Taylor, T. Otanicar, A review of nanofluid-based direct absorption solar collectors: design considerations and experiments with hybrid PV/Thermal and direct steam generation collectors, *Renew. Energy* 145 (2020) 903–913, <https://doi.org/10.1016/j.renene.2019.06.097>.
- [33] Z. Xu, C. Kleinstreuer, Concentration photovoltaic-thermal energy co-generation system using nanofluids for cooling and heating, *Energy Convers. Manag.* 87 (2014) 504–512, <https://doi.org/10.1016/j.enconman.2014.07.047>.
- [34] D. DeJarnette, N. Brekke, E. Tunkara, P. Hari, K. Roberts, T. Otanicar, Design and feasibility of high temperature nanoparticle fluid filter in hybrid thermal/photovoltaic concentrating solar power, *High Low Concentrator Syst. Solar Energy Appl.* X 9559 (2015), 95590C, <https://doi.org/10.1117/12.2186117>.
- [35] M.S. Selim, H. Yang, F.Q. Wang, X. Li, Y. Huang, N.A. Fathallah, Silicone/Ag@SiO<sub>2</sub> core-shell nanocomposite as a self-cleaning antifouling coating material, *RSC Adv.* 8 (18) (2018) 9910–9921, <https://doi.org/10.1039/c8ra00351c>.
- [36] R. Lee, J.B. Kim, C. Qin, H. Lee, B.J. Lee, G.Y. Jung, Synthesis of Terminol-based plasmonic nanofluids with core/shell nanoparticles and characterization of their absorption/scattering coefficients, *Sol. Energy Mater. Sol. Cell.* 209 (2020), 110442, <https://doi.org/10.1016/j.solmat.2020.110442>. February.
- [37] J. Walsh, P.M. Carron, C. McLoughlin, S. McCormack, J. Doran, G. Amarandi, Nanofluid development using silver nanoparticles and organic-luminescent molecules for solar-thermal and hybrid photovoltaic-thermal applications, *Nanomaterials* 10 (2020), <https://doi.org/10.3390/nano10061201>.
- [38] M. Chaabane, W. Charfi, H. Mhiri, P. Bournot, Performance evaluation of concentrating solar photovoltaic and photovoltaic/thermal systems, *Sol. Energy* 98 (PC) (2013) 315–321, <https://doi.org/10.1016/j.solener.2013.09.029>.
- [39] W. Charfi, M. Chaabane, H. Mhiri, P. Bournot, Performance evaluation of a solar photovoltaic system, *Energy Rep.* 4 (2018) 400–406, <https://doi.org/10.1016/j.egypr.2018.06.004>.
- [40] S. Dubey, J.N. Sarvaiya, B. Seshadri, Temperature dependent photovoltaic (PV) efficiency and its effect on PV production in the world - a review, *Energy Proc.* 33 (2013) 311–321, <https://doi.org/10.1016/j.egypro.2013.05.072>.
- [41] M. Chaabane, W. Charfi, H. Mhiri, P. Bournot, Performance evaluation of concentrating solar photovoltaic and photovoltaic/thermal systems, *Sol. Energy* 98 (PC) (2013) 315–321, <https://doi.org/10.1016/j.solener.2013.09.029>.
- [42] G.M. Hale, M.R. Querry, Optical constants of water in the 200-nm to 200- $\mu$ m wavelength region, *Appl. Opt.* 12 (3) (1973) 555, <https://doi.org/10.1364/AO.12.000555>.
- [43] H. Buiteveld, J.H.M. Hakvoort, M. Donze, Optical Properties of Pure Water, 2258, *SPIE Ocean Optics XII*, 1994, pp. 174–183, <https://doi.org/10.1117/12.190060>.
- [44] H. Tyagi, P. Phelan, R. Prasher, Predicted efficiency of a Low-temperature Nanofluid-based direct absorption solar collector, *J. Solar Energy Eng. Trans. ASME* 131 (4) (2009), <https://doi.org/10.1115/1.3197562>, 0410041–0410047.
- [45] Y. Khetib, H.M. Abo-Dief, A.K. Alanazi, G. Cheraghian, S.M. Sajadi, M. Sharifpur, Simulation of nanofluid flow in a micro-heat sink with corrugated walls considering the effect of nanoparticle diameter on heat sink efficiency, *Front. Energy Res.* 9 (November) (2021) 1–11, <https://doi.org/10.3389/feeng.2021.769374>.
- [46] H. Ghorabae, M.R.S. Emami, F. Moosakazemi, N. Karimi, G. Cheraghian, M. Afrand, The use of nanofluids in thermosyphon heat pipe: a comprehensive review, *Powder Technol.* 394 (2021) 250–269, <https://doi.org/10.1016/j.powtec.2021.08.045>.
- [47] M.W. Tian, et al., Energy, exergy and economics study of a solar/thermal panel cooled by nanofluid, *Case Stud. Therm. Eng.* 28 (2021), 101481, <https://doi.org/10.1016/j.csite.2021.101481>.

- [48] C.F. Bohren, Absorption and Scattering of Light by Small Particles, " *Absorption And Scattering of Light by Small Particles*, 1983, <https://doi.org/10.1088/0031-9112/35/3/025>.
- [49] R.A. Taylor, P.E. Phelan, T.P. Otanicar, R. Adrian, R. Prasher, Nanofluid optical property characterization: towards efficient direct absorption solar collectors, *Nanoscale Res. Lett.* 6 (1) (2011) 1–11, <https://doi.org/10.1186/1556-276X-6-225>.
- [50] P.B. Johnson, R.W. Christy, Optical constant of the noble metals, *Phys. Rev. B* 6 (12) (1972) 4370–4379.
- [51] J. Choi, et al., Optical dielectric constants of single crystalline silver films in the long wavelength range, *Opt. Mater. Express* 10 (2) (2020) 693, <https://doi.org/10.1364/ome.385723>.
- [52] G. Rosenblatt, B. Simkhovich, G. Bartal, M. Orenstein, Nonmodal plasmonics: controlling the forced optical response of nanostructures, *Phys. Rev. X* 10 (1) (2020), 11071, <https://doi.org/10.1103/PhysRevX.10.011071>.
- [53] R.L. Olmon, et al., Optical dielectric function of gold, *Phys. Rev. B Condens. Matter* 86 (23) (2012) 1–9, <https://doi.org/10.1103/PhysRevB.86.235147>.
- [54] Y. Tripanagnostopoulos, M. Souliotis, ICS solar systems with two water tanks, *Renew. Energy* 31 (11) (2006) 1698–1717, <https://doi.org/10.1016/j.renene.2005.08.028>.